Vol. 8 (2015) *Acta Physica Polonica B Proceedings Supplement* No 4

MEASUREMENT OF THE JET PRODUCTION PROPERTIES AT THE LHC WITH THE ATLAS DETECTOR*

Stanislav Tokar

on behalf of the ATLAS Collaboration

Comenius University in Bratislava, Mlynská dolina F1, 842 48 Bratislava, Slovakia

(Received November 12, 2015)

Different features of the jet production in pp collisions at $\sqrt{s} = 7$ TeV have been measured by the ATLAS experiment. Among them are: the dijet double-differential cross sections, upper limit of the scale for contact interaction, the flavor dijet decomposition for different light-, c-, and b-jet combinations, double-differential inclusive jet cross sections, and b-jet and light-jet shapes measured using top-quark pair events. In all cases, good agreement with the SM QCD expectations was found. The dijet analysis provided a lower limit for the compositeness scale of about 7 TeV.

DOI:10.5506/APhysPolBSupp.8.949

PACS numbers: 12.38.Aw, 12.38.Bx, 12.38.Lg, 12.39.Hg

1. Introduction

Measurements of jet production in proton–proton (pp) collisions at the LHC [1] test the predictions of Quantum Chromodynamics (QCD) at the largest energies explored so far in collider experiments. Under QCD, jets are the result of fragmentation of partons produced in a scattering process. In high-energy particle collisions, there are two main phases: perturbative phase where partons with high-transverse momenta (p_{T}) are produced in a hard-scattering process, and non-perturbative phase with partons converting into hadrons. All these aspects of high energy collisions are probed in the jet physics. Study of flavour of jets, especially those originating from charm (c) and bottom (b) quarks, is important as the heavy flavour jets are expected to be described well by perturbative QCD (pQCD) calculations. This work deals with studies of jet processes in pp collisions at $\sqrt{s} = 7$ TeV collected by the ATLAS experiment [2].

* Presented at EDS Blois 2015: The 16$^{\mathrm{th}}$ Conference on Elastic and Diffractive Scattering, Borgo, Corsica, France, June 29–July 4, 2015.

2. Event and jet selection and reconstruction

In analyses discussed here, different selection procedures were used. Typically, a set of single-jet triggers with different thresholds was used to collect data and only events with at least one primary vertex were taken. Primary vertex with the highest $\sum p_{\mathrm{T}}^2$ of associated tracks was selected as the hard-scattering vertex. Jets were reconstructed by the anti-k_{t} algorithm and clustered using two different values of jet radius parameter R: 0.4 and 0.6. The measured jet distributions were corrected for all experimental effects and were defined at the particle-level final state. Here, particle level refers to stable particles (a lifetime longer than 10 ps, including muons and neutrinos) — for details, see Ref. [3]. The measured unfolded cross sections are compared to next-to-leading-order (NLO) QCD predictions which are corrected for non-perturbative effects in fragmentation process and in underlying event, and for NLO electroweak effects.

3. Results

The following jet physics topics measured by the ATLAS experiment are presented here: the dijet cross sections, limits on contact interaction, dijet flavour decomposition, inclusive jet cross section, three-jet production and jet shapes in $t\bar{t}$ events. All the mentioned topics were studied in pp collisions at the centre-of-mass energy $\sqrt{s} = 7$ TeV.

Dijet production. ATLAS measured the double-differential dijet cross sections as functions of the dijet mass and half the rapidity separation of the two highest-p_{T} jets, $y^\star = 0.5|y_1 - y_2|$ [4]. The leading (subleading) jet is required to have $p_{\mathrm{T}} > 100$ GeV ($p_{\mathrm{T}} > 50$ GeV). The measurement is made in six ranges of $y^\star < 3.0$, in equal steps of 0.5. The measured cross sections are defined at the particle-level final state. The analysis was performed using data collected at $\sqrt{s} = 7$ TeV corresponding to an integrated luminosity of 4.5 fb^{-1}. Figure 1 shows dijet double-differential cross sections for jets with radius parameter $R = 0.4$ as a function of dijet mass in different ranges of $y^\star$. The data are compared with the NLO QCD predictions of NLOJET++ [5] using the CT10 PDF set which are corrected for non-perturbative and electroweak effects. As it follows from Fig. 1, the data are in a very good agreement with the predictions. Detailed quantitative comparisons between the measured cross sections and theoretical predictions have been carried out in Ref. [4]. Good agreement was observed when using the CT10, NNPDF2.1, and MSTW 2008 PDF (parton distribution functions) sets[1] for the theoretical predictions with values of the jet radius parameter $R = 0.4$ and $R = 0.6$. Disagreement was observed in some ranges of dijet mass and $y^\star$ when using

[1] References to the PDF sets can be found in Ref. [4].

the HERAPDF1.5 PDF set, for both values of the jet radius parameter, and for the NLOJET++ predictions using the ABM11 PDF set, indicating sensitivity of the measurements to the choice of PDF set.

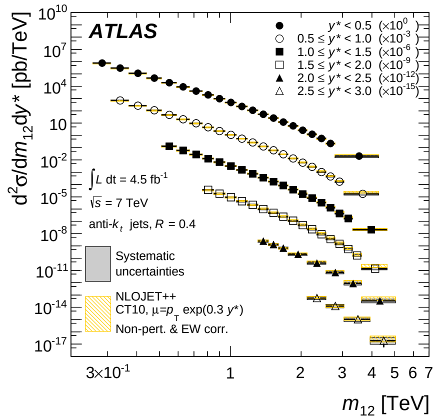

Fig. 1. Dijet differential cross sections for jets with radius $R = 0.4$ is shown as a function of dijet mass in different ranges of $y^\star$ (from [4]).

Using measured cross sections, the CLs technique [6] has been employed to explore possible deviations in dijet production due to contributions of the beyond SM physics. An exclusion limit for a model of contact interactions was found, computed using full NLO QCD. An exclusion of compositeness scales $\Lambda < 6.9$–7.7 TeV has been obtained, depending on the PDF set used for the calculation.

Dijet flavour decomposition. In the study described in Ref. [7], ATLAS performed a measurement of the flavour composition of dijet events. Fractions of six dijet flavour states were extracted: BB, CC, UU, BU, CU, BC, where U stands for light, C for charm and B for bottom jet. The analysis was performed using the data set of an integrated luminosity of 39 nb^{-1}. Selected events are required to have at least one reconstructed primary vertex candidate. Jets are reconstructed using the anti-k_{t} algorithm with a jet radius parameter $R = 0.4$ and only jets with a transverse momentum of $p_{\mathrm{T}} > 30$ GeV and a rapidity of $|y| < 2.1$ are considered. The two jets with highest p_{T} are required to have an angular separation in azimuth of $\Delta\varphi > 2.1$ rad (a back-to-back topology). To distinguish jet flavour, two kinematic variables were chosen

$$\varPi = \frac{m_{\mathrm{vert}} - 0.4}{m_B} \frac{\sum_{\mathrm{vert}} E_i}{\sum_{\mathrm{jet}} E_i}\,, \qquad B = \frac{\sqrt{m_B}\, \sum_{\mathrm{vert}} \vec{p_{\mathrm{T}}}_i}{m_{\mathrm{vert}}\, \sqrt{p_{\mathrm{T\,jet}}}}\,, \tag{1}$$

where m_{vert} is the invariant mass of the particles associated with the vertex,

E ($\vec{p}_{\rm T}$) is the energy (transverse momentum) of individual track, m_B = 5.2794 GeV is the average B-meson mass and each sum indicates whether the summation is performed over particles associated with secondary vertex or jet. The analysis results are shown in Fig. 2 which shows the unfolded dijet flavour fractions for six leading jet $p_{\rm T}$ bins, compared with PYTHIA 6.423 [8], Herwig++ 2.4.2 [9] and POWHEG [10] + PYTHIA 6.423 predictions. From Fig. 2, it follows that except for the BU case, all data fractions are in agreement with the predictions of the LO and NLO generators.

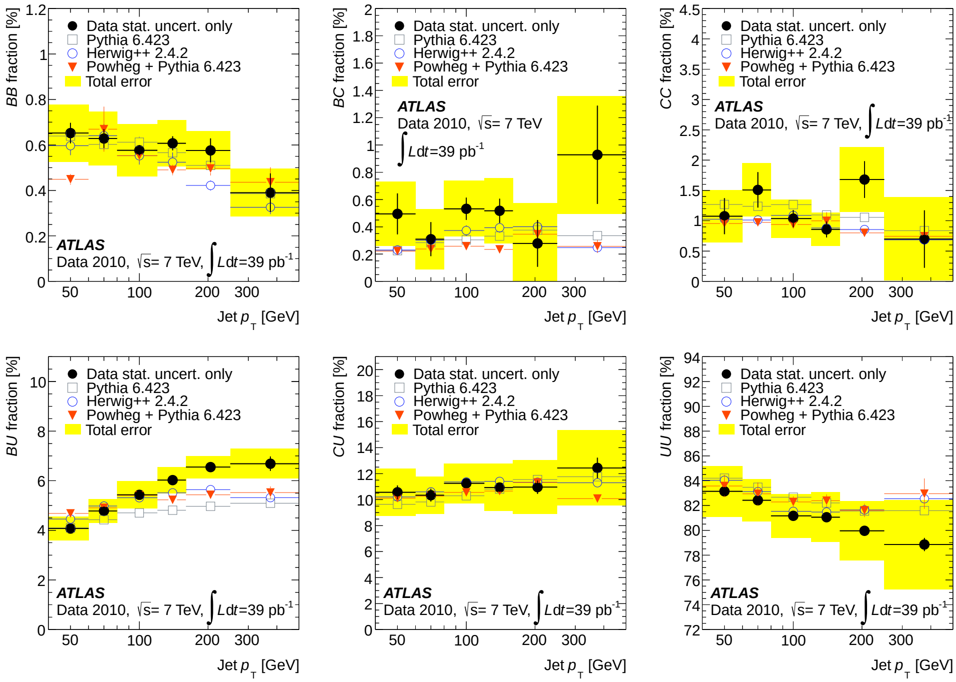

Fig. 2. The unfolded dijet flavour fractions for six leading jet $p_{\rm T}$ bins (black points) with PYTHIA 6.423 (squares), Herwig++ 2.4.2 (circles) and POWHEG+PYTHIA 6.423 (filled triangles) predictions overlaid (from [7]).

Inclusive jet cross sections at 7 TeV. Measurement of differential inclusive jet cross sections, in addition to the test of validity of pQCD, enables to probe the proton PDFs. ATLAS measured these differential cross sections at $\sqrt{s} = 7$ TeV using a data set corresponding to an integrated luminosity of 4.5 fb^{-1}. The double-differential cross sections were measured as a function of the jet transverse momentum in six jet rapidity bins, and unfolded to the particle level. These cross sections are compared with NLO QCD calculations for different PDF sets corrected for non-perturbative and electroweak effects (see Ref. [11]) and with MC simulations using NLO matrix elements interfaced to parton showering. Ratios of the NLO pQCD predictions to the measured cross sections were found for the predictions using the NLO PDF sets CT10, MSTW 2008, NNPDF 2.1, HERAPDF1.5, and ABM 11. As an example, a comparison of the ratios for the predictions using the NLO PDF sets CT10, MSTW 2008, and NNPDF 2.1 is presented in Fig. 3. The predictions are generally consistent with the measured cross sections for jets with both radius parameter values, though the level of consistency varies among the predictions with the different PDF sets — for details, see Ref. [11].

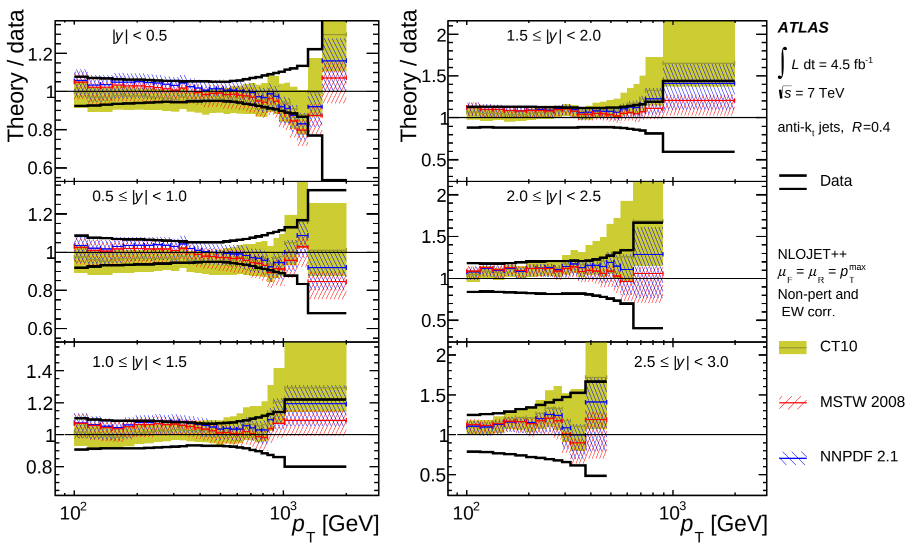

Fig. 3. Ratio of NLO pQCD predictions to the measured double-differential inclusive jet cross section, shown as a function of the jet p_{T} in bins of the jet rapidity, for anti-k_{t} jets with $R = 0.4$. The predictions are calculated using NLOJET++ with different NLO PDF sets, namely CT10, MSTW2008 and NNPDF 2.1 (from [11]).

Three-jet production cross sections. A motivation for the three-jet cross section measurement is to study higher order effects in jet production. ATLAS performed measurements of double-differential three-jet production cross sections presented as a function of the three-jet invariant mass (m_{jjj}) and the sum of absolute rapidity separation between the three leading jets ($|Y^{\star}| = |y_1 - y_2| + |y_2 - y_3| + |y_1 - y_3|$) [12]. The measured cross sections were corrected for experimental effects and reported at the particle level. Data are selected by a jet-trigger system which is fully efficient in events with a leading jet passing the three-jet analysis requirements. Events containing at least three jets within the rapidity range $|y| < 3.0$ with $p_{\mathrm{T}} > 50$ GeV were selected. The leading, subleading and sub-subleading jets are required to have $p_{\mathrm{T}} > 150$ GeV, $p_{\mathrm{T}} > 100$ GeV, and $p_{\mathrm{T}} > 50$ GeV, respectively.

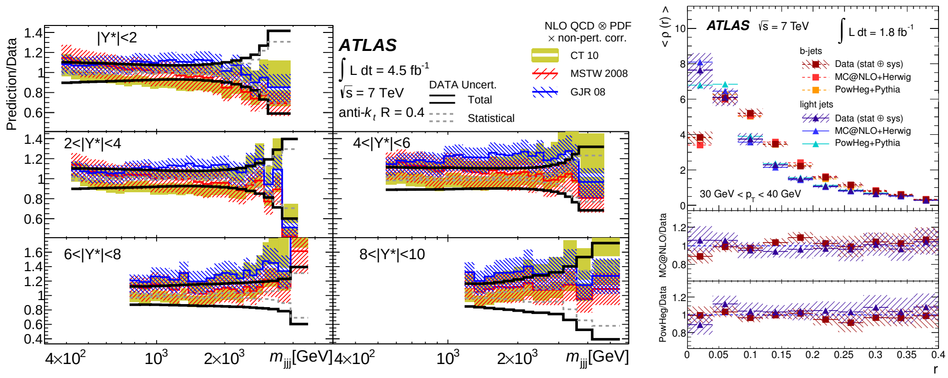

Fig. 4. Left (from [12]): the ratio of NLO QCD predictions, obtained by using NLOJET++ with different PDF sets (CT 10, MSTW 2008, GJR 08), to data as a function of m_{jjj} in 5 bins of $|Y^\star|$. Right (from [13]): the differential jet shapes $\langle\rho(r)\rangle$ for light jets (triangles) and b-jets (squares) as a function of r compared to MC@NLO+Herwig and POWHEG+PYTHIA predictions.

The measured double-differential three-jet cross sections were compared to the NLO QCD calculations using NLOJET++ with the CT 10 PDF set corrected for non-perturbative effects. Good agreement between the data and the theoretical predictions was found. As an example, in Fig. 4 (left), ratios of the theoretical predictions calculated with various PDF sets to the measured cross sections for the $R = 0.4$ jets are presented.

Jet shapes in $t\bar{t}$ events. Hadronic jets are theoretically interpreted to arise from partons — quarks (q) and gluons (g) produced in deep inelastic interactions. The internal structure of a jet is expected to depend primarily on the type of parton it originated from. ATLAS measured the differential and integral jet shapes in top-quark pair events using 1.8 fb^{-1} at $\sqrt{s} = 7$ TeV [13]. The differential jet shape $\rho(r)$ in an annulus of inner radius $r - \Delta r/2$ and outer radius $r + \Delta r/2$ from the axis of a given jet is defined as

$$\rho(r) = \frac{1}{\Delta r}\,\frac{p_{\mathrm{T}}\,(r - \Delta r/2, r + \Delta r/2)}{p_{\mathrm{T}}(0, R)}\,, \tag{2}$$

where $\Delta r = 0.04$ is the annulus width, r is the distance to jet axis in the η–ϕ plane, and $p_{\mathrm{T}}(r_1, r_2)$ is the scalar sum of the p_{T} of the jet constituents with radii between r_1 and r_2. The integrated jet shape in a cone of radius $r \le R$ around the jet axis is defined as the cumulative distribution for $\rho(r)$.

In Fig. 4 (right), as an example, the distributions for the average values of the differential jet shapes are shown for p_{T} bin of 30–40 GeV, along with a comparison with the NLO expectations from the simulated samples. As can be seen from Fig. 4 (right), there is a clear difference between light- and b-jet differential shapes. The observed jet shapes are in good agreement with the theoretical expectations from MC@NLO [14] and POWHEG+PYTHIA.

4. Summary

Jet physics provides us with powerful means for testing of QCD. The ATLAS experiment has measured many features of the jet physics in pp collisions. Some of the measurements performed at $\sqrt{s} = 7$ TeV are reported here. Among them, there are the dijet differential cross sections — using the dijet events, the scale of contact interaction was excluded below 7 TeV. Flavour dijet decomposition for different light-, c-, and b-jet combinations were measured. The differential inclusive jet cross section measurement as a function of jet p_{T} and rapidity was performed. Using $t\bar{t}$ events, the b-jet and light-jet shapes were measured as a function of the distance to the jet axis and jet p_{T}. In all the listed cases, good agreement with the SM QCD expectations has been found.

REFERENCES

[1] L. Evans, P. Bryant, *JINST* **3**, S08001 (2008).
[2] The ATLAS Experiment at the CERN LHC, *JINST* **3**, S08003 (2008).
[3] ATLAS Collaboration, *Eur. Phys. J. C* **75**, 17 (2015).
[4] ATLAS Collaboration, *J. High Energy Phys.* **1405**, 059 (2014).
[5] Z. Nagy, *Phys. Rev. D* **68**, 094002 (2003) [arXiv:hep-ph/0307268].
[6] A.L. Read, *J. Phys. G* **28**, 2693 (2002).
[7] ATLAS Collaboration, *Eur. Phys. J. C* **73**, 2301 (2013).
[8] T. Sjostrand, S. Mrenna, P.Z. Skands, *J. High Energy Phys.* **0605**, 026 (2006) [arXiv:hep-ph/0603175].
[9] M. Bahr *et al.*, *Eur. Phys. J. C* **58**, 639 (2008) [arXiv:0803.0883 [hep-ph]].
[10] S. Alioli *et al.*, *J. High Energy Phys.* **1104**, 081 (2011) [arXiv:1012.3380 [hep-ph]].
[11] ATLAS Collaboration, *J. High Energy Phys.* **1502**, 153 (2015) [*Erratum ibid.* **1509**, 141 (2015)].
[12] ATLAS Collaboration, *Eur. Phys. J. C* **75**, 228 (2015).
[13] ATLAS Collaboration, *Eur. Phys. J. C* **73**, 2676 (2013).
[14] S. Frixione *et al.*, *J. High Energy Phys.* **1101**, 053 (2011) [arXiv:1010.0568 [hep-ph]].